Particle Accelerators, 1993, Vol. 41, pp 133–151
Reprints available directly from the publisher
Photocopying permitted by license only

DIFFUSION IN A FODO CELL DUE TO MODULATION EFFECTS IN THE PRESENCE OF NON-LINEAR FIELDS

OLIVER S. BRÜNING

DESY, 2 Hamburg 52, Germany

Received 19 October 1992, in final form 8 December 1992

Looking at the simple model structure of a long FODO cell with one sextupole kick, we study the effect of tune modulation in the presence of sextupole nonlinearities for one and two modulation frequencies. For the frequency regime of 9 Hz - 900 Hz, we show three different mechanisms which lead to a drastic increase in the emittance growth for a tune modulation with two, rather than one modulation frequency. In all three cases, the increase in the emittance growth has a non-linear dependence on the modulation depth due to an overlap of modulation sidebands.

1 INTRODUCTION

A recent experiment at the SPS[1] concentrated on the nonlinear-beam-dynamics in the presence of strong nonlinear multipoles and tune modulation. The nonlinearities were generated by strong sextupole magnets and three different frequencies were used for the tune modulation. An interesting result of the experiment was that the particle diffusion due to the tune modulation could be enhanced by using two, rather than only one modulation frequency. Because the same net modulation amplitude was used for both cases, the experiment clearly indicates a diffusion due to the nonlinear character of the beam-dynamics. The authors in Ref. 1 suggest an explanation of the observed effects by an overlap of neighbouring resonance sidebands. (For an introduction to the effect of resonance overlap and its impact on the particle diffusion, we refer to Ref. 2 or Ref. 3 and the literature cited in Ref. 2.)

In this paper we will investigate the combined effect of tune modulation and sextupole nonlinearities in detail. In particular, we are interested in the sideband structure and a possible sideband overlap due to the tune modulation. In our analysis we look at a long FODO cell with only one sextupole kick and assume that all particles lie inside some volume V_{beam} around the origin of the transversal phase space. Our model structure has five dominating resonances in the horizontal phase space, all of which lie outside of the volume V_{beam}. In the following, we will assume that the particle diffusion is entirely determined by the horizontal resonances, which implies that the vertical emittance is much smaller than the horizontal. In the absence of tune modulation we do not observe any substantial emittance growth during the first $2.0 \cdot 10^6$ passages through the FODO cell. In the presence of tune modulation however, we observe a particle diffusion with

the same characteristics as those observed in the SPS experiment. The emittance growth for a tune modulation with two frequencies is much larger than in the case of a tune modulation with one frequency only.

The tune modulation leads to resonance sidebands of the five dominating resonances. The particle diffusion due to these sidebands depends entirely on the number, strength, and position (overlap) of the sidebands which reach into the volume V_{beam}. For a fast tune modulation ($f = O(100\text{Hz})$), the distance of neighbouring sidebands is large, but the amplitudes decrease very rapidly with increasing order. A fast tune modulation might therefore lead only to a small number of well-separated sidebands which reach into the volume V_{beam}. For a slow tune modulation ($f = O(1\text{Hz})$), one observes the opposite behavior. The distance of neighbouring sidebands is small and the amplitudes decrease only slowly with increasing order. However, the sidebands cannot spread over large distances of the phase space. A slow tune modulation might therefore lead to a rich structure of sidebands, but no sidebands with a significant amplitude which can reach into the volume V_{beam}. Both modulation cases lead therefore only to a very slow emittance growth.

For the case of a tune modulation with two frequencies, three effects lead to an increased diffusion. First, in the case of a tune modulation with a fast and a slow frequency, the sidebands of the fast modulation frequency act as resonance seeds for the slow modulation frequency, i.e. the slow tune modulation leads to a rich structure of sidebands around the sidebands of the fast modulation. As a result, we expect a large number of resonance sidebands with non vanishing amplitudes inside the volume V_{beam}, and hence, an increased emittance growth. Second, in the case of a tune modulation with two approximately equal frequencies, the number of resonance sidebands increases and the sidebands of the two modulation frequencies might overlap. As a result, the sidebands that reach into the volume V_{beam} will result in a significant emittance growth. Third, a tune modulation with any two frequencies increases the widths of the stochastic layers related to the resonance sidebands.

The paper is organized as follows. First we derive the Hamilton function of a FODO cell with sextupole kick and harmonic tune modulation in action-angle variables[3] and calculate the nonlinear detuning due to the sextupole kick with the help of Deprit perturbation theory.[3,4] In the second part we construct the corresponding nonlinear map and calculate the mode amplitudes for the resonances that appear in sixth order perturbation theory or lower. In this calculation, we use the nonlinear map for particle tracking and derive the mode amplitudes from the numerically determined resonance widths. Third, using these mode amplitudes, we analyse the sideband structure in the presence of tune modulation and estimate modulation frequencies which lead to an extremely fast emittance growth. We present numerical data that shows an enhanced particle diffusion for a tune modulation with the estimated frequencies.

2 THE HAMILTON FUNCTION

The linear motion of an on-momentum particle in a FODO structure is governed by Hill's equation,[5] i.e., linear equations with periodic coefficients:

$$\frac{d^2x}{ds^2} = -K_x(s)\cdot x; \qquad \frac{d^2z}{ds^2} = -K_z(s)\cdot z. \tag{1}$$

s is the distance along the equilibrium orbit and x and z are the horizontal and vertical displacements of the particle from the equilibrium orbit, respectively. Introducing action-angle variables via the canonical transformation

$$F_1 = -\sum_{y=x,z} \frac{y^2}{2\beta_y(s)} \cdot \{\tan(\Phi_y + \Phi_{y,0}) + \alpha_y(s)\}, \tag{2}$$

the corresponding Hamilton function takes the convenient form

$$H = \nu_x \cdot I_x + \nu_z \cdot I_z. \tag{3}$$

ν_x and ν_z are the horizontal and vertical tunes, and for simplicity we assume constant beta functions: $\beta_y(s) = 1/\nu_y$, $\rightarrow \alpha_y \equiv 0$[5] ($y = x, z$).

Introducing the potential for the sextupole kick[6]

$$V(x,z,s) = \delta_L(s)\cdot\frac{\lambda}{6}\cdot(x^3 - 3xz^2), \tag{4}$$

and a horizontal tune modulation with N frequencies, the Hamilton function (3) takes the form

$$\begin{aligned} H \;=\; & \nu_x \cdot \left[1 + \sum_{p=1}^{N} a_p \cdot \cos\left(\frac{2\pi\Omega_p}{L}\cdot s\right)\right]\cdot I_x + \nu_z \cdot I_z + \\ & \frac{\lambda}{L\cdot 3\sqrt{8}}\cdot\sqrt{\beta_x\cdot I_x}^{\,3}\cdot\sum_{k=-\infty}^{+\infty}\left\{3\cdot\cos\left(\phi_x + \frac{2\pi}{L}\cdot k\cdot s\right) + \right. \\ & \left. + \cos\left(3\phi_x + \frac{2\pi}{L}\cdot k\cdot s\right)\right\} - \\ & \frac{\lambda}{L\cdot 3\sqrt{8}}\cdot\sqrt{\beta_x\cdot I_x}\cdot\beta_z\cdot I_z\cdot\sum_{k=-\infty}^{+\infty}\left\{6\cdot\cos\left(\phi_x + \frac{2\pi}{L}\cdot k\cdot s\right) + \right. \\ & \left. 3\cdot\cos\left(\phi_x - 2\cdot\phi_z + \frac{2\pi}{L}\cdot k\cdot s\right) + 3\cdot\cos\left(\phi_x + 2\cdot\phi_z + \frac{2\pi}{L}\cdot k\cdot s\right)\right\}. \end{aligned} \tag{5}$$

λ is the integrated sextupole strength ($\lambda = \frac{e}{P_0}\int_0^L \left(\frac{\partial^2 B_z}{\partial x^2}\right)_{x=z=0} ds \rightarrow [\lambda] = \frac{1}{m^2}$), B the magnetic field, e the unit charge, L the length of the FODO cell, P_0 the particle momentum, and $\delta_L(s)$ is the periodic delta function ($\delta_L(s) = \sum_m \delta(s - m\cdot L)$).

Finally, we use the canonical transformation

$$F_2 = \tilde{I}_x \cdot \left[\phi_x - \sum_{p=1}^{N} \frac{a_p \nu_x L}{2\pi\Omega_p} \cdot \sin\left(\frac{2\pi\Omega_p}{L} \cdot s \right) \right], \tag{6}$$

in order to eliminate the tune modulation from the linear part of (5) and get

$$\begin{aligned} H \;=\; & \nu_x \cdot \tilde{I}_x + \nu_z \cdot \tilde{I}_z + \frac{2\varepsilon}{3 \cdot L} \cdot \sqrt{\beta_x \cdot \tilde{I}_x}^{\,3} \cdot \\ & \sum_{k,\vec{n}} \left\{ \left[\prod_{p=1}^{N} J_{n_p}\left(\frac{a_p \nu_x L}{2\pi\Omega_p} \right) \right] \cdot 3 \cdot \cos\left(\tilde{\phi}_x + \frac{2\pi}{L} \cdot (k + \vec{n} \cdot \vec{\Omega}) \cdot s \right) + \right. \\ & \left. \left[\prod_{p=1}^{N} J_{n_p}\left(\frac{3 a_p \nu_x L}{2\pi\Omega_p} \right) \right] \cdot \cos\left(3\tilde{\phi}_x + \frac{2\pi}{L} \cdot (k + \vec{n} \cdot \vec{\Omega}) \cdot s \right) \right\} - \\ & \frac{2\varepsilon}{3 \cdot L} \cdot \sqrt{\beta_x \cdot \tilde{I}_x} \cdot \beta_z \cdot \tilde{I}_z \cdot \sum_{k,\vec{n}} \left[\prod_{p=1}^{N} J_{n_p}\left(\frac{a_p \nu_x L}{2\pi\Omega_p} \right) \right] \cdot \\ & \left\{ 6 \cdot \cos\left(\tilde{\phi}_x + \frac{2\pi}{L} \cdot (k + \vec{n} \cdot \vec{\Omega}) \cdot s \right) + \right. \\ & 3 \cdot \cos\left(\tilde{\phi}_x - 2 \cdot \tilde{\phi}_z + \frac{2\pi}{L} \cdot (k + \vec{n} \cdot \vec{\Omega}) \cdot s \right) + \\ & \left. 3 \cdot \cos\left(\tilde{\phi}_x + 2 \cdot \tilde{\phi}_z + \frac{2\pi}{L} \cdot (k + \vec{n} \cdot \vec{\Omega}) \cdot s \right) \right\}, \end{aligned} \tag{7}$$

where we have introduced the small parameter $\varepsilon = \frac{\lambda}{2\sqrt{8}}$, the vectors $\vec{n} = (n_1, ..., n_N)$ and $\vec{\Omega} = (\Omega_1, ..., \Omega_N)$, and where $J_{n_p}\left(\frac{a_p \nu_x L}{2\pi\Omega_p} \right)$ are the Bessel functions of the first kind.

Using perturbation theory,[3] Hamiltonian (7) can be written in the general form

$$H = \sum_{\alpha,\beta,l,m,k,\vec{n}} \varepsilon^{(\alpha+\beta-2)} \cdot A_{\alpha,\beta,l,m,k,\vec{n}} \cdot \hat{I}_x^{\alpha/2} \cdot \hat{I}_z^{\beta/2} \cdot e^{i\left(l \cdot \hat{\phi}_x + m \cdot \hat{\phi}_z + \frac{2\pi}{L} \cdot \left(k + \vec{n} \cdot \vec{\Omega} \right) s \right)}. \tag{8}$$

Neglecting all the vertical Fourier-modes but the nonlinear detuning terms and the coupling mode of the horizontal and vertical motion, (8) takes the form

$$H = H_x + H_z + H_{x,z} \tag{9}$$

with

$$\begin{aligned} H_x \;=\; & \nu_x \cdot \hat{I}_x + \frac{1}{2}\varepsilon^2 \cdot \nu_{x,2} \cdot \hat{I}_x^2 + \frac{1}{3}\varepsilon^3 \cdot \nu_{x,4} \cdot \hat{I}_x^3 + \\ & \sum_{\alpha,k,l,\vec{n}} \varepsilon^{(\alpha-2)} \cdot A_{x,\alpha,l,k,\vec{n}} \cdot \hat{I}_x^{\alpha/2} \cdot e^{i\left(l \cdot \hat{\phi}_x + \frac{2\pi}{L} \cdot \left(k + \vec{n} \cdot \vec{\Omega} \right) s \right)} \end{aligned} \tag{10}$$

$$H_z = \nu_z \cdot \hat{I}_z + \frac{1}{2}\varepsilon^2 \cdot \nu_{z,2} \cdot \hat{I}_z^2 \tag{11}$$

$$H_{x,z} = \varepsilon^2 \cdot \nu_{xz,2} \cdot \hat{I}_x \cdot \hat{I}_z + \varepsilon^2 \cdot A_{x,z} \cdot \hat{I}_x \cdot \hat{I}_z \cdot \cos\left(2 \cdot \hat{\phi}_x - 2 \cdot \hat{\phi}_z\right), \tag{12}$$

where we have introduced the notation $\nu_{x,2}$, $\nu_{z,2}$, $\nu_{xz,2}$, and $\nu_{x,4}$ for the nonlinear detuning of the sextupole in second and fourth order perturbation theory. It is this Hamilton function that lies at the heart of our paper. In the following analysis we will look at the horizontal motion (10) as the driving term for the diffusion of the vertical emittance I_z. This mechanism dominates the diffusion as long as $I_x \gg I_z$. [7]

For the following analysis we choose

$Q_x = 25.158$	$Q_z = 25.252$	$L = 47.018 \cdot 10^2$ m
$\lambda = 3.0\text{m}^{-2}$		$P_0 = 820\text{GeV/c}$,

(13)

with $\nu_x = \frac{2\pi}{L} \cdot Q_x$ and $\nu_z = \frac{2\pi}{L} \cdot Q_z$. L is 100 times the HERA-p FODO cell length, $P_0 c$ is the HERA-p design energy, and λ is about 8% of the sextupole strength of the sextupole correction coils in these 100 HERA-p FODO cells.[8] Furthermore, we will characterize the horizontal resonances with the corresponding parameter vector $(\alpha, l, k, \vec{n})$, where α, l, k, and $\vec{n}$ are taken from the expanded Hamiltonian (8). $(\alpha + 2)$ describes the order in the perturbation series in which the resonance appears, l and k specify the mode of the horizontal the longitudinal motion respectively, and $\vec{n}$ specifies the modulation sideband.

In order to treat the diffusion analytically we have to estimate the nonlinear detuning terms, the horizontal resonance amplitudes $A_{x,\alpha,k,l,n}$, and the coupling mode amplitude $A_{x,z}$ in (10), (11), and (12). For the calculation of the detuning terms and the coupling mode amplitude, we used a computer algorithm based on Deprit perturbation theory,[3,4] and get

$\varepsilon^2 \cdot \tilde{\nu}_{x,2} = -9.0\text{m}^{-2}$	$\varepsilon^2 \cdot \tilde{\nu}_{z,2} = -10.0\text{m}^{-2}$
$\varepsilon^2 \cdot \tilde{\nu}_{xz,2} = +11.6\text{m}^{-2}$	$\varepsilon^4 \cdot \tilde{\nu}_{x,4} = -0.12 \cdot 10^7\text{m}^{-3}$
$\lvert A_{x,z} \rvert \approx 35.39\text{m}^2$.	

(14)

For the calculation of the horizontal resonance amplitudes, we insert (13) and (14) into $\frac{\partial H_x}{\partial \hat{I}_x}$ and calculate the stable and unstable fixed points $\hat{\phi}_{x_0,k}$ and $\hat{I}_{x_0,k}$ for the resonance of interest. After transforming these coordinates back to the initial variables $I_{x_0,k}$ and $\phi_{x_0,k}$, we use the fixed point coordinates as the initial conditions for an iterative application of the nonlinear map corresponding to (5). From the numerical data we can finally evaluate the resonance amplitudes. In the next section we will construct the nonlinear map necessary for this calculation.

3 NONLINEAR MAPPING

In this section we will construct the one-turn-map corresponding to the Hamilton function (5) and present numerical data obtained by an iterative application of this map. The numerical data is used for the construction of the surfaces of section, for the determination

of the resonance amplitudes, and for the calculation of the particle diffusion under the influence of one and two modulation frequencies.

The linear equation of motion corresponding to the Hamilton function (5) without sextupole kick can be integrated, yielding

$$\begin{aligned} I_x((h+1)\cdot L) &= I_x(h\cdot L), & I_z((h+1)\cdot L) &= I_z(h\cdot L) \\ \phi_x((h+1)\cdot L) &= \phi_x(h\cdot L)+\triangle_x(h\cdot L), & \phi_z((h+1)\cdot L) &= \phi_z(h\cdot L)+\triangle_z, \end{aligned} \tag{15}$$

with

$$\begin{aligned} \triangle_x(h\cdot L) &= \nu_x\cdot L+\sum_{p=1}^{N}\left[\frac{a_p\nu_x L}{\pi\Omega_p}\cdot\sin(\pi\Omega_p)\cdot\cos\left(2\pi\Omega_p\cdot(h+\frac{1}{2})\right)\right] \\ \triangle_z &= \nu_z\cdot L. \end{aligned} \tag{16}$$

Taking into account the sextupole kick (4) and transforming back to the variables $x, P_x, z,$ and P_z, the position after the $(h+1)^{th}$ passage through the FODO cell can be expressed as a function of the position after the h^{th} passage through the FODO cell via a successive application of the linear transfer map

$$\begin{pmatrix} \tilde{x} \\ \tilde{P}_x \\ \tilde{z} \\ \tilde{P}_z \end{pmatrix}_{h+1} = \begin{pmatrix} a_{1,x} & a_{2,x} & 0 & 0 \\ a_{3,x} & a_{4,x} & 0 & 0 \\ 0 & 0 & a_{1,z} & a_{2,z} \\ 0 & 0 & a_{3,z} & a_{4,z} \end{pmatrix} \cdot \begin{pmatrix} x \\ P_x \\ z \\ P_z \end{pmatrix}_h \tag{17.a}$$

with

$$a_{1,y}=a_{4,y}=\cos(\triangle_y),\quad a_{2,y}=-a_{3,y}\cdot\beta_y^2=\beta_y\cdot\sin(\triangle_y),\quad y=x,z,$$

and the sextupole kick

$$\begin{pmatrix} x \\ P_x \\ z \\ P_z \end{pmatrix}_{h+1} = \begin{pmatrix} \tilde{x} \\ \tilde{P}_x \\ \tilde{z} \\ \tilde{P}_z \end{pmatrix}_{h+1} + \begin{pmatrix} 0 \\ -\frac{\lambda}{2}\cdot(\tilde{x}_{h+1}^2-\tilde{z}_{h+1}^2) \\ 0 \\ \lambda\cdot\tilde{x}_{h+1}\cdot\tilde{z}_{h+1} \end{pmatrix} \tag{17.b}$$

to the particle coordinates.

We will use this combined map for the construction of the surface of section (SoS) for the horizontal particle motion ($I_z\equiv 0,\quad \phi_z\equiv 0$). We choose the surface $s=\kappa\cdot L$ for the surface of section, with $\kappa\in\mathbf{Z}$ imposed by the map (17). For the construction of the SoS, one has to limit the tune modulation to frequencies that satisfy the resonance condition

$$\gamma+\vec{\delta}\cdot\vec{\Omega}=0;\qquad \gamma,\delta_p\in\mathbf{Z};\quad \mathrm{p}=1,2,..,\mathrm{N};\qquad \rightarrow_{\mathrm{p}}=\frac{\mathrm{q}}{\mathrm{r}},\ \mathrm{q},\mathrm{r}\in\mathbf{Z}. \tag{18}$$

Rather than taking the particle coordinates after each passage through the FODO structure, as in the case without tune modulation, we take the coordinates now only after each κ^{th}

passage through the FODO structure, with κ being the smallest common denominator of the Ω_p. Without this restriction, we can only construct a stroboscopic phase space projection, which does not depict the clear resonance island structure necessary for a calculation of the resonance widths.

Fig. 1 shows the SoS without tune modulation. The upper part of Fig. 1 shows the SoS in the x, P_x variables and the right-hand side shows the SoS in the action angle variables (ϕ_x, I_x). The island structures of the $(5, 7, -175, \vec{0})$, $(6, 8, -201, \vec{0})$, and $(5, 9, -226, \vec{0})$ resonances are clearly recognizable. With the help of the SoS, we can measure the resonance widths of the resonance sidebands and calculate the resonance amplitudes. For the calculation of the mode amplitudes, we change to resonance variables

$$F_2 = \bar{I}_x \cdot \left(l \cdot \hat{\phi}_x + \frac{2\pi}{L} \cdot (k + \vec{n} \cdot \vec{\Omega}) \cdot s \right) \tag{19}$$

and expand (10) into a Taylor series around a stable resonance fixed point $\bar{I}_{+res}$ of the map. Recognizing that the absolute value of the resonance half width $\triangle \bar{I}_{1/2}$ is always much smaller than the fixed point value $\bar{I}_{x,res}$, we get the following relation between the mode amplitudes and the measured resonance widths:

$$|A_{\alpha,k,l,\vec{n}}| = \left| \frac{\triangle \hat{I}_{1/2}^2 \cdot (\nu_{x,2} + 2 \cdot \hat{I}_x \cdot \nu_{x,4})}{4 \cdot \varepsilon^{(\alpha-2)} \cdot \hat{I}_{x,res}^{\alpha/2}} \right|. \tag{20}$$

Table (21) shows the resulting resonance amplitudes for resonances up to 6^{th} order perturbation theory.

Resonances in 1^{st} order perturbation theory:	
$A_{3,k,1,\vec{0}} = 0.07\mathrm{m}^{1/2}$	$A_{3,k,3,\vec{0}} = 0.023\mathrm{m}^{1/2}$
Resonances in 2^{nd} order perturbation theory:	
$A_{4,-151,6,\vec{0}} = 0.05\mathrm{m}^2$	
Resonances in 3^{rd} order perturbation theory:	
$A_{5,-176,7,\vec{0}} = 60.0\mathrm{m}^{7/2}$	$A_{5,-226,9,\vec{0}} = 85.0\mathrm{m}^{7/2}$
Resonances in 4^{th} order perturbation theory:	
$A_{6,-201,8,\vec{0}} = 2.0 \cdot 10^4\mathrm{m}^5$	
Resonances in 6^{th} order perturbation theory:	
$A_{8,-352,14,\vec{0}} = 1.0 \cdot 10^{10}\mathrm{m}^8$	

(21)

All other resonances are either too far away from the dynamic aperture for their sidebands to reach into the volume V_{beam}, or their amplitudes are so small that we will neglect them in the following analysis.

Before we use the map (17) for a calculation of the particle diffusion, we will discuss the sideband structure arising from the tune modulation.

4 THE SIDEBAND STRUCTURE

Now, that we have constructed the Hamilton function and its corresponding nonlinear map for our model structure, we are ready to examine the tune modulation and its effect

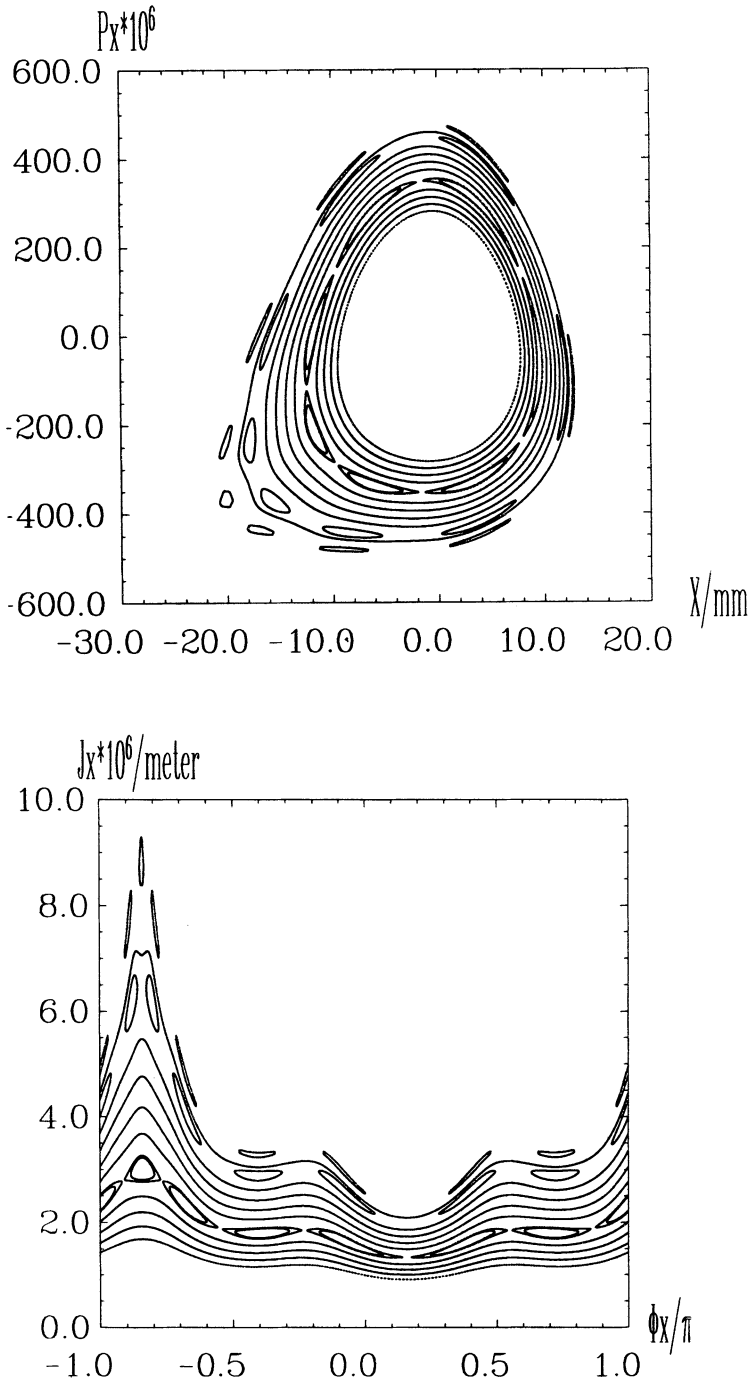

FIGURE 1: The surfaces of section without tune modulation. One clearly recognizes the islands of three of the five dominating sextupole resonances.
Top: The SoS in the P_x and x variables. Bottom: The SoS in the action angle variables.

on the emittance growth. First, we will look at the Hamilton function (10) in order to understand the structure of the modulation sidebands. In a second step, we will use the gained insight into the sideband structure and estimate modulation frequencies which result in an increased emittance growth, and finally, we will illustrate the effects with numerical data from an iterative application of the map (17).

In the following, we will limit our analysis to the case of one and two modulation frequencies, and assume that all particles lie within the volume V_{beam}, given by

$$\begin{aligned} 4.0 \cdot 10^{-7}\mathrm{m} \leq \quad I_x \quad &\leq 10.0 \cdot 10^{-7}\mathrm{m}, \\ 0.9 \cdot 10^{-7}\mathrm{m} \leq \quad I_z \quad &\leq 1.0 \cdot 10^{-7}\mathrm{m}. \end{aligned} \tag{22}$$

We start our analysis with the Hamiltonian (10) and derive a closed expression for the mode amplitudes. For this, we neglect the $\vec{\Omega}$ term in the denominator

$$\frac{1}{l \cdot \nu_x + \frac{2\pi}{L} \cdot \left[k + \vec{n} \cdot \vec{\Omega}\right]},$$

which appears in the Deprit perturbation theory. This approximation is good as long as the linear tune ν_x is not close to a resonance

$$l \cdot L\nu_x + 2\pi \cdot k = 0,$$

and as long as

$$l \cdot L\nu_x + 2\pi \cdot \left[k + \vec{n} \cdot \vec{\Omega}\right] \not\ll L, \quad \text{for} \quad \mathrm{n_p} \lesssim \frac{\mathrm{a_p} \cdot \nu_\mathrm{x} \cdot \mathrm{L}}{2\pi_\mathrm{p}}.$$

In this approximation, we get for the mode amplitudes

$$A_{x,\alpha,k,l,\vec{n}} = \left[\prod_{p=1}^{N} J_{n_p}\left(\frac{l \cdot a_p \cdot \nu_x \cdot L}{2\pi\Omega_p}\right)\right] \cdot A_{x,\alpha,k,l,\vec{0}}. \tag{23}$$

Equation (23) implies that all sidebands with

$$|n_p| > |\frac{la_p\nu_x L}{2\pi\Omega_p}|$$

have a vanishing amplitude and can hence be neglected in the diffusion analysis. We test (23) for a modulation frequency of 875 Hz ($\rightarrow \Omega = 1/70$). Looking at (23), we expect a vanishing amplitude for the ($l = 7, n = 0$) resonance for $a = 1.9 \cdot 10^{-4}$, because the Bessel function $J_0(z)$ has a root for $z = 2.4$. The numerical data obtained with the nonlinear map (17) yields $a = 1.6 \cdot 10^{-4}$, which is in good agreement with the value predicted by (23).

In order to calculate the resonance values for the horizontal action, we solve the fixed point equations

$$\frac{\partial H}{\partial \hat{I}_x} = 0, \quad -\frac{\partial H}{\partial \hat{\phi}_x} = 0$$

for $\hat{I}_{x,res}$ and get

$$\hat{I}_{x,res} = -\left[\nu_x + \frac{2\pi}{l \cdot L} \cdot \left(k + \vec{n} \cdot \vec{\Omega}\right)\right] / \nu_{x,2}. \tag{24}$$

Equation (24) shows that a slow modulation frequency leads to a small, and that a fast modulation frequency leads to a large spacing of neighbouring sidebands.

First, we discuss the effect of a tune modulation with one fast and one slow modulation frequency. The Hamilton function (10) has five dominating resonances, all of which lie outside the volume V_{beam}:

$(\alpha = 4, l = 6, k = -150, \vec{n} = \vec{0})$	$\hat{I}_{x,6} \approx 1.0 \cdot 10^{-5}$ m
$(\alpha = 5, l = 7, k = -176, \vec{n} = \vec{0})$	$\hat{I}_{x,7} \approx 2.0 \cdot 10^{-6}$ m
$(\alpha = 5, l = 9, k = -226, \vec{n} = \vec{0})$	$\hat{I}_{x,9} \approx 6.3 \cdot 10^{-6}$ m
$(\alpha = 6, l = 8, k = -201, \vec{n} = \vec{0})$	$\hat{I}_{x,8} \approx 4.4 \cdot 10^{-6}$ m
$(\alpha = 8, l = 14, k = -353, \vec{n} = \vec{0})$	$\hat{I}_{x,14} \approx 7.5 \cdot 10^{-6}$ m.

(25)

The tune modulation leads to resonance sidebands of these five resonances. For a fast tune modulation ($f = O(100\text{Hz})$), the distance of neighbouring sidebands is large (see Eq. (24)), and mode amplitudes decrease very rapidly with increasing order n_p (see Eq. (23)). Hence, a fast tune modulation might only lead to a small number of well-separated sidebands which reach into the volume V_{beam}. For a slow tune modulation ($f = O(1\text{Hz})$), the behaviour is reversed. The distance of neighbouring sidebands is small, and the amplitudes decrease only slowly with increasing order n_p. A slow tune modulation might lead to a rich structure of sidebands, but no sidebands with a significant amplitude which can reach into the volume V_{beam}. Both modulation cases lead therefore only to a very slow emittance growth. For the case of a tune modulation with a fast and a slow frequency, the situation changes drastically. The sidebands of the fast modulation frequency act as resonance seeds for the slow modulation frequency, i.e. the slow tune modulation leads to a rich structure of sidebands around the sidebands of the fast modulation. As a result, we expect a large number of resonance sidebands with non-vanishing amplitudes inside the volume V_{beam}, and hence, an increased emittance growth.

In order to illustrate this seeding effect, we add the resonance widths of all modulation sidebands of the five resonances (25) which lie inside the volume V_{beam}. Figure 2 shows the quotient of the total volume covered by the modulation sidebands

$$V_{res} = \sum_{I_{x,(\alpha,l,k,\vec{n})} \in V_{beam}} \triangle_{1/2} \hat{I}_{x,\alpha,l,k,\vec{n}} \tag{26}$$

and the volume V_{beam} occupied by the particles as a function of the modulation frequencies. The solid line shows the relative volume for a tune modulation with one frequency only, and the dashed line shows the relative volume for a modulation with two frequencies. For the latter, the slow modulation frequency was kept at 9 Hz (the slowest modulation frequency used in the SPS experiment) and only the second frequency was varied. In both cases, the net modulation depth was $a = 2.0 \cdot 10^{-4}$, which corresponds to $\triangle Q_x \approx 5.0 \cdot 10^{-3}$ and is approximately twice the modulation depth used in the SPS experiment. Figure 2 shows clearly that the relative volume V_{res}/V_{beam} is approximately

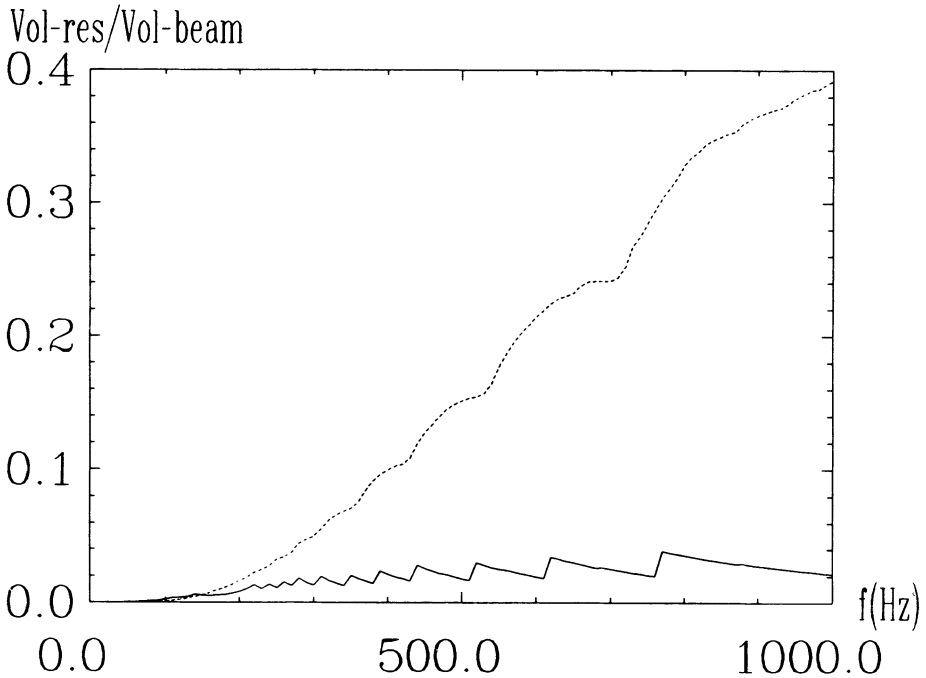

FIGURE 2: The quotient of the volume covered by resonance islands V_{res} and the volume occupied by the beam V_{beam} vs. the modulation frequency.
The solid line shows the quotient for one modulation frequency only and the dashed line shows the quotient for two modulation frequencies. For the latter, the slow modulation frequency was kept at 9Hz. One clearly sees the dramatic increase of the quotient for a tune modulation with one slow and one fast frequency.

14 times larger for a modulation with 9 Hz and 750 Hz than for any single modulation frequency, and suggests a drastic increase of the particle diffusion due to an increased number of resonances inside the volume V_{beam} and due to an overlap of resonance sidebands. Qualitatively, one observes the same effect for any modulation depth, but the volume gain becomes smaller with decreasing modulation depth.

In the next step, we will measure the specific effect of the tune modulation on the particle diffusion. We use a Gaussian distribution in the action variables and look at 3000 particles with initial conditions inside the volume V_{beam}. We track the particles for three different tune modulations through our model structure and assume a horizontal and vertical aperture limitation of $\pm 40.0m$ m for the x and z variables. First, we consider a modulation depth of $a = 2.0 \cdot 10^{-4}$ and a single frequency modulation of 9Hz ($\rightarrow \Omega_1 = 1/6200$) and 875Hz ($\rightarrow \Omega = 1/70$). For both frequencies, we have no particle loss due to tune modulation over the first $2.0 \cdot 10^6$ turns, and observe a vertical emittance growth of less than 3%. The upper part of Fig. 3 shows the vertical emittance as a function of the number of turns for $f = 875$ Hz. Second, we look at a simultaneous tune modulation with both frequencies, each having a modulation depth $a = 1.0 \cdot 10^{-4}$.

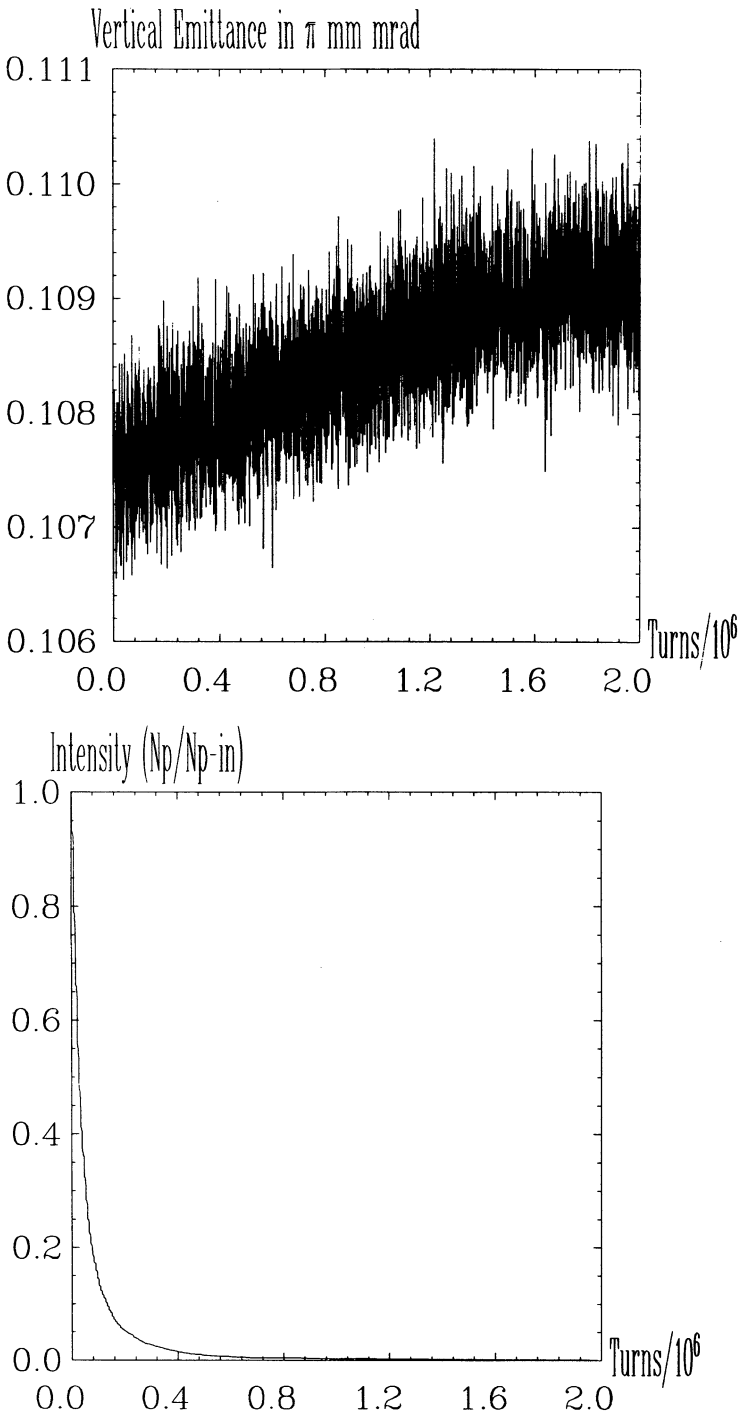

FIGURE 3: Illustration of the effect of a tune modulation with one slow and one fast frequency. For a tune modulation with one frequency we observe only a small increase in the vertical emittance. The upper part shows the vertical emittance vs. the number of turns for $f = 875$ Hz. For a tune modulation with two extremely different frequencies we observe a drastic increase in the vertical emittance. The lower part shows the normalized number of particles vs. the number of turns for $f_1 = 9$ Hz and $f_2 = 875$ Hz.

Although we have the same net modulation depth as in the previous case, we now lose all 3000 particles during the first $2.0 \cdot 10^6$ turns. The lower part of Fig. 3 shows the normalized number of particles versus the number of turns. The drastic increase in the particle loss nicely illustrates the seeding effect for a tune modulation with a slow and a fast frequency.

Next, we analyse the tune modulation with two approximately equal frequencies. We choose for example

$$f_1 = 875\text{Hz}(\rightarrow \Omega_1 = 1/70), \qquad f_2 = 766\text{Hz}(\rightarrow \Omega_2 = 1/80),$$

and look at the location of the resonance sidebands. For $f = 875$ Hz the smallest non-negative action for the $(4, 6, -151, n)$ resonance according to (24) is given by

$$\hat{I}_{x,(4,6,-151,5)} \approx 2.8 \cdot 10^{-7}\text{m} \tag{27}$$

and has a sideband spacing of

$$\triangle \hat{I}_{x,res} \approx 3.0 \cdot 10^{-7}\text{m}. \tag{28}$$

As a result, only the (n=6) and (n=7) sidebands of the $(\alpha = 4, l = 6, k = -151)$ resonance lie inside the volume V_{beam}. For a modulation depth of $a = 4.0 \cdot 10^{-4}$, which corresponds to $\triangle Q_x = O(10^{-2})$ and which is approximately five times the modulation depth of the SPS experiment, the resonance width given by (20) is approximately $3.0 \cdot 10^{-9}$ m. The $(n = 6)$ and $(n = 7)$ sidebands cannot overlap and cover only a small fraction of the volume V_{beam}. Consequently, we expect only a small diffusion of the particles. If we consider on the other hand a simultaneous tune modulation with both frequencies and with the same net modulation depth, the situation is quite different. For the $(4, 6, -151, \vec{n})$ resonance, we get now for the sideband spacing

$$\triangle \hat{I}_{x,res} \approx 4.0 \cdot 10^{-8}\text{m} \tag{29}$$

The small sideband spacing has two main effects. First, the number of sidebands reaching into the volume V_{beam} increases, and second, neighbouring sidebands might now overlap. Because the condition for sideband overlap depends on the resonance widths of the sidebands, we expect the existence of a critical modulation depth above which the resonance overlap occurs. If we neglect the fourth order detuning term in (20), solve for $\triangle I_{1/2}$, and substitute (23) into (20), we get for the resonance width of the sidebands

$$\triangle I_{1/2} \approx \sqrt{\frac{4\varepsilon^{(\alpha-2)} \cdot I_{x,res}^{\alpha/2} \cdot J_{n_1}\left(\frac{la_1\nu_x L}{2\pi\Omega_1}\right) \cdot J_{n_2}\left(\frac{la_2\nu_x L}{2\pi\Omega_2}\right) \cdot A_{\alpha,k,l}}{\nu_{x,2}}}. \tag{30}$$

Two neighbouring sidebands overlap if

$$\triangle I_{1/2}(\alpha, l, k, \vec{n}) + \triangle I_{1/2}(\tilde{\alpha}, \tilde{l}, \tilde{k}, \tilde{\vec{n}}) > \triangle \hat{I}_{res}. \tag{31}$$

For $I_{x,res} < 1.0 \cdot 10^{-6}$, $a_1 = a_2$, $f_1 = 875$ Hz, and $f_2 = 766$ Hz, we get for example

$$a_{min} \approx 1.5 \cdot 10^{-4}. \tag{32}$$

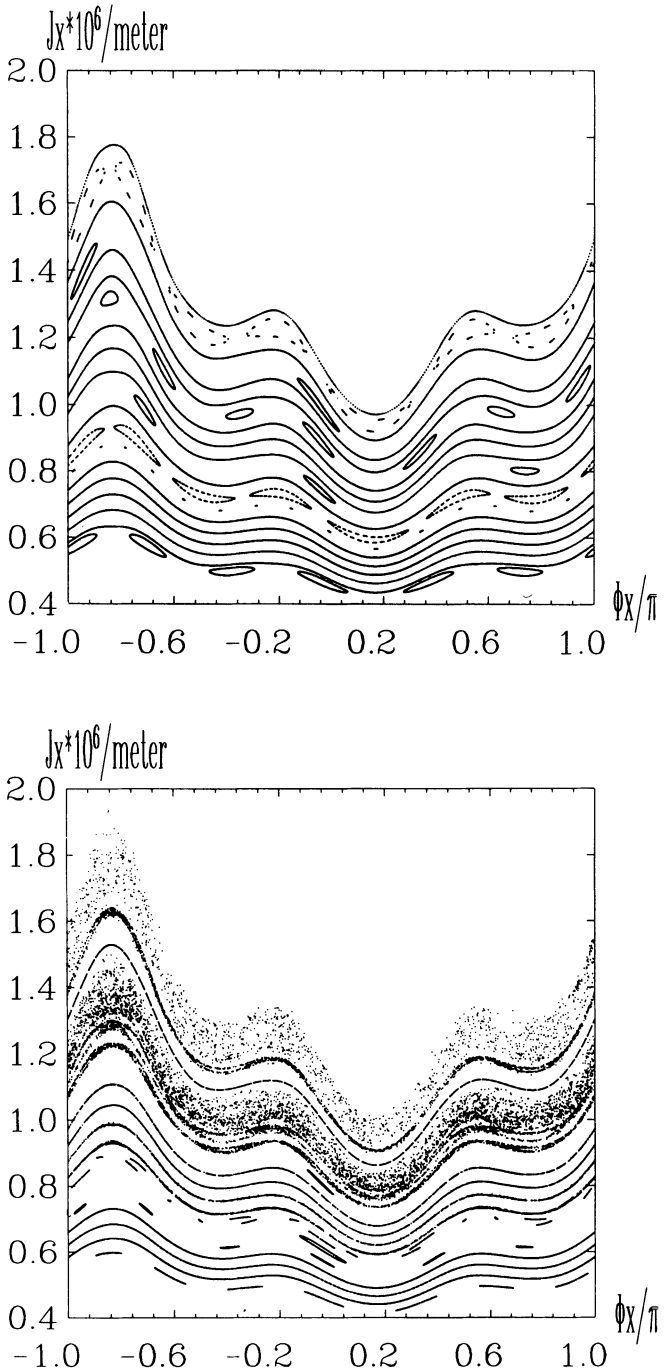

FIGURE 4: Illustration of the effect of a tune modulation with two approximately equal frequencies. The upper part shows the surface of section in action-angle variables for a tune modulation with $f = 875$ Hz. The lower part shows surface of section for a tune modulation with $f_1 = 9$ Hz and $f_2 = 875$ Hz and the same net modulation depth. One clearly recognizes the appearance of new resonance sidebands.

For modulation depths smaller than a_{min}, we expect no sideband overlap for any of the five dominating sextupole resonances (21). For modulation depths larger than this critical modulation depth, the modulation sidebands might overlap and we expect a large particle diffusion. For the following numerical analysis we choose $a_1 = a_2 = 2.0 \cdot 10^{-4}$. Figure 4 shows the SoS for the horizontal motion in the presence of tune modulation. The upper part of Fig. 4 shows the SoS for $\Omega_{mod} = \frac{1}{70}$ and $a = 4.0 \cdot 10^{-4}$ and the lower part of Fig. 4 shows the SoS for $\Omega_1 = \frac{1}{70}$, $a_1 = 2.0 \cdot 10^{-4}$ and $\Omega_2 = \frac{1}{80}$, $a_2 = 2.0 \cdot 10^{-4}$. One clearly sees the appearance of new resonance sidebands and the stochastic layers due to an overlap of the sidebands for a tune modulation with two frequencies. Again, we will measure the effect of a tune modulation on the particle diffusion for both frequencies. For the tracking, we choose again a Gaussian distribution in the actions with the initial coordinates inside the volume V_{beam}. For the tune modulation with one frequency only and with $a = 4.0 \cdot 10^{-4}$, we do not lose any particles due to tune modulation during the first $2.0 \cdot 10^6$ turns. However, for the simultaneous modulation with both frequencies and with the same net modulation depth, we lose 65% of the particles during the first $2.0 \cdot 10^6$ turns. The lower part of Fig. 5 shows the normalized number of particles versus the number of turns for the simultaneous modulation with both frequencies, each with $a_p = 2.0 \cdot 10^{-4}$.

In order to demonstrate the dependence of the diffusion on the modulation depth, and in order to illustrate the qualitative difference between the modulation with two approximately equal frequencies and the resonance seeding of a slow and a fast frequency, we look at a simultaneous tune modulation with the same frequencies ($f_1 = 875$Hz, $f_2 = 766$Hz), but each with half the modulation depth $a_p = 1.0 \cdot 10^{-4}$, which lies below the critical depth a_{min}. With this smaller modulation depth, the emittance growth is smaller than 3% and in contrast to the modulation with $a_p = 2.0 \cdot 10^{-4}$, we do not lose any particles due to the tune modulation. The upper part of Fig. 5 shows the vertical emittance versus the number of turns for $a_p = 1.0 \cdot 10^{-4}$. Eventhough the emittance growth changed drastically, the relative volume V_{res}/V_{beam} is still of the same order for both cases,

$$V_{res}/V_{beam}(a_p = 1.0 \cdot 10^{-4}) \approx 0.1, \; V_{res}/V_{beam}(a_p = 2.0 \cdot 10^{-4}) \approx 0.3,$$

which is qualitatively different from the tune modulation with one slow and one fast modulation frequency.

The last effect in our discussion of the tune modulation is the widening of the stochastic layers. Looking at one resonance island of a sextupole resonance sideband, we see that the tune modulation might be in resonance with the island oscillation frequency. The islands of such a resonance are depicted in the upper part of Fig. 6. Figure 6 shows the SoS of the horizontal motion in action angle variables and with a modulation frequency $\Omega = 1/84$. Inside the island of the $(5, 7, -151, \vec{0})$ sextupole resonance we see three smaller islands surrounding the stable fixed point of the $(5, 7, -151, \vec{0})$ resonance. If we take the particle coordinates after each passage through the FODO structure, we obtain a stroboscopic projection of the phase space trajectory on to the horizontal phase space. In such a stroboscopic projection, the coordinates circulate around the stable fixed point of the $(5, 7, -151, \vec{0})$ resonance.

For the fixed points of the three smaller islands, the revolution frequency is related to

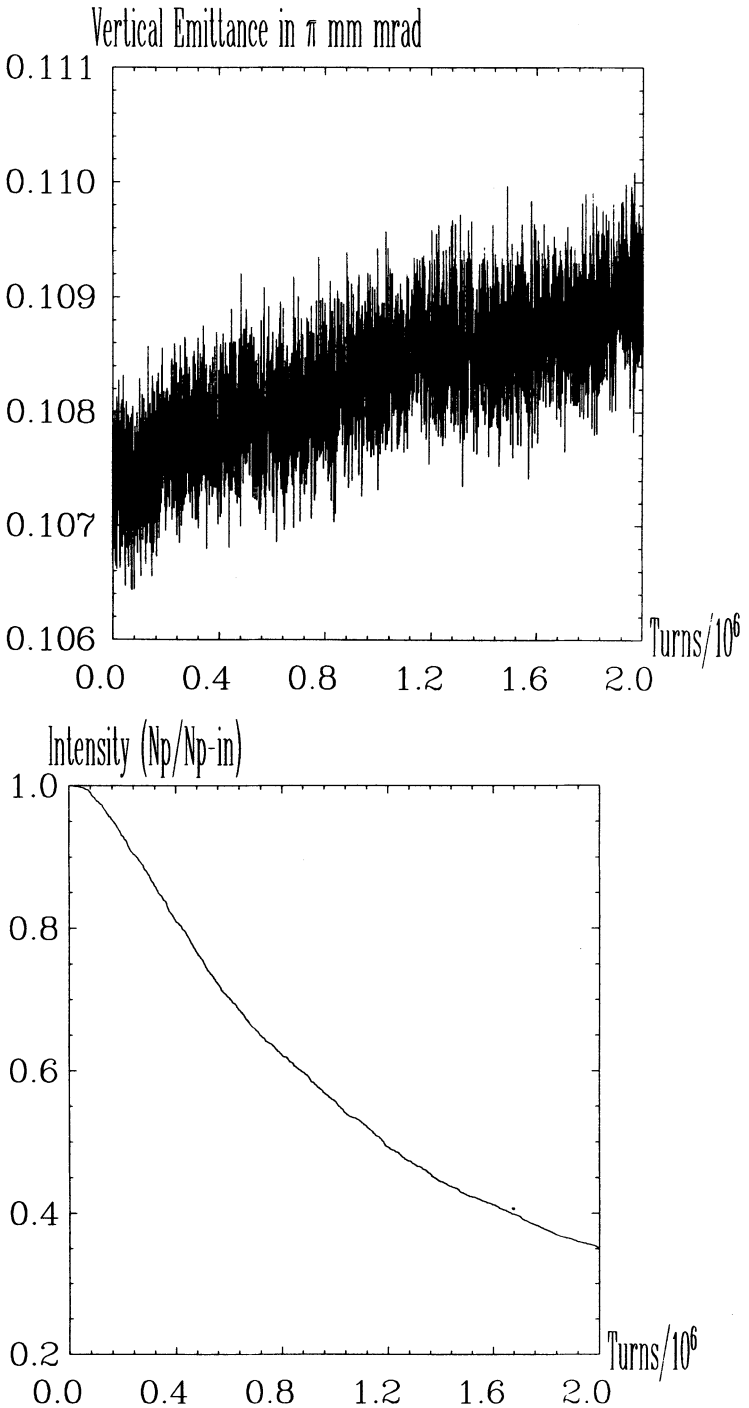

FIGURE 5: Illustration of the nonlinear dependence of the emittance growth on the modulation depth. In both pictures we look at a tune modulation with two frequencies.
Top: For a total modulation depth of $\triangle Q \approx 2.5 \cdot 10^{-3}$, we observe only a small emittance growth of approximately 3%.
Bottom: For a total modulation depth of $\triangle Q \approx 5.0 \cdot 10^{-3}$, we lose almost 70% of the particles during the first $2 \cdot 10^6$ turns.

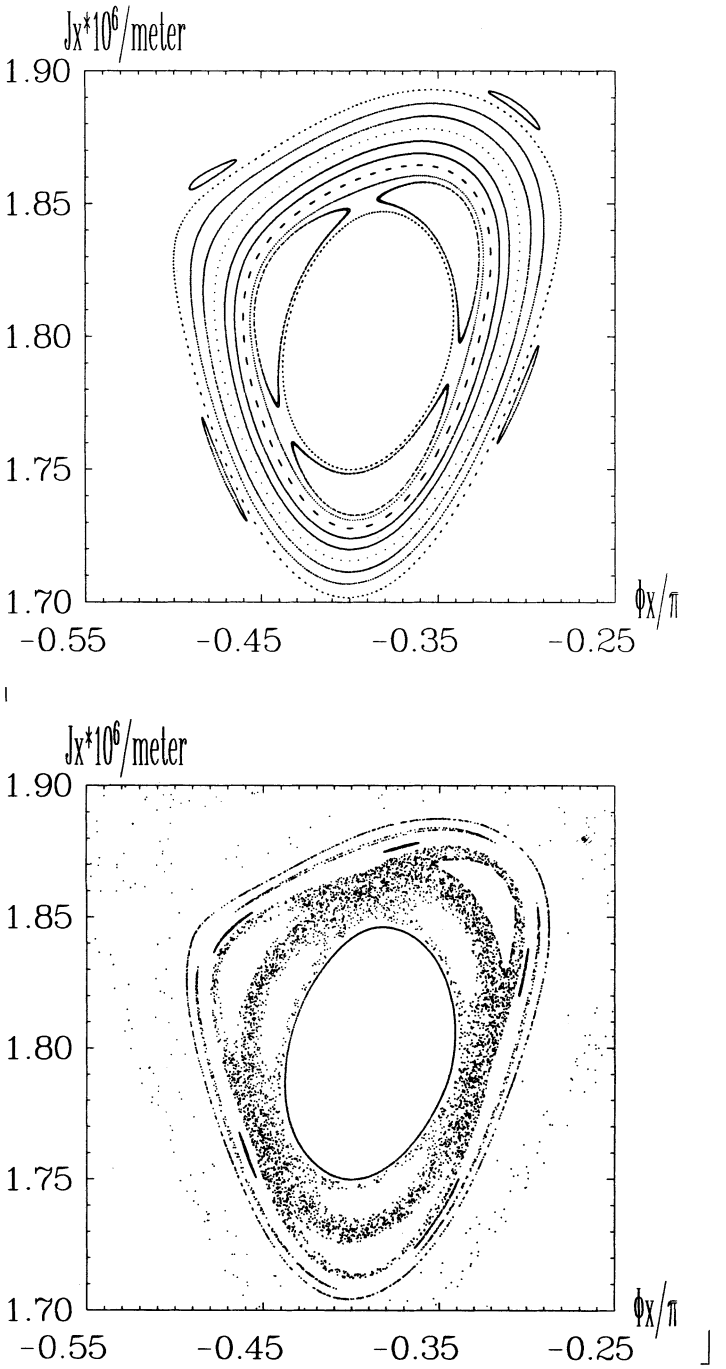

FIGURE 6: Illustrating the widening of the chaotic layer due to an overlap of neighbouring modulation resonances.
Top: Modulation with $\Omega_1 = 1/84$.
Bottom: Modulation with $\Omega_1 = 1/84$ and $\Omega_2 = 1/91$.

the modulation frequency by

$$\Omega_o = \Omega_{mod}/3.$$

Therefore, the observed resonance islands in the sextupole resonance correspond to a resonance between the island oscillation frequency of the $(5, 7, -151, \vec{0})$ sextupole resonance and the modulation frequency $\Omega = 1/84$. In the following, we will call a resonance with N islands an N^{th}-order modulation resonance. Because the period of the island oscillation increases as the trajectory approaches the separatrix of the sextupole resonance $(\Omega_o \to 0)$,[3] the number of resonance islands inside the sextupole resonance increases as well. In the vicinity of the separatrix, the resonance islands overlap and lead to a wider stochastic layer as in the case of no tune modulation. For a modulation with more than one frequency, modulation resonances of the different modulation frequencies can overlap even if they are not close to the separatrix of the sextupole resonance. This overlap of modulation resonances of different modulation frequencies leads to a widening of the stochastic layers related to the sextupole sideband resonances, and is depicted in the lower part of Fig. 6 for $\Omega_1 = 1/84$, $\Omega_2 = 1/91$, and $a_p = 2.0 \cdot 10^{-6}$.

5 SUMMARY

Looking at the simple model structure of a long FODO cell with one sextupole kick, we studied the effect of tune modulation in the presence of sextupole nonlinearities. For modulation frequencies and modulation depths of the same order of magnitude as in the SPS experiment ($f = 9\text{Hz} \leftrightarrow 800\text{Hz}$, $\triangle Q = 1.0 \cdot 10^{-3} \leftrightarrow 5.0 \cdot 10^{-3}$), we were able to reproduce the effects observed in the SPS. For a tune modulation with two frequencies the vertical emittance growth was much larger than for a tune modulation with one frequency only. The simple nature of our model structure could be used to nicely illustrate the different effects which lead to an increased vertical emittance growth. Our analysis showed three qualitatively different effects.

In the case of a tune modulation with one fast and one slow frequency, the sidebands of the fast modulation act as resonance seeds for the slow tune modulation. Consequently, the area accessible to the beam is densely covered with resonance sidebands and we expect an increased particle diffusion. This increase of the number of resonance sidebands reaching into the area accessible to the beam can be easily recognized by looking at the quotient of the total volume covered by resonance islands (V_{res}) and the volume covered by the beam (V_{beam}). For the case of two extremely different modulation frequencies (for example $f_1 = 9$ Hz and $f_2 = 875$ Hz) the quotient V_{res}/V_{beam} was 14 times larger as in the case of two approximately equal frequencies or any single modulation frequency. The expected increase in the particle diffusion was verified by particle tracking.

In the case of a modulation with two approximately equal frequencies, we observed an overlap of neighbouring resonance sidebands which was extremely sensitive to the modulation depth. Below a critical modulation depth, neighbouring resonance sidebands can not overlap and the diffusion decreases drastically. We illustrated this second effect for $f_1 = 766$ Hz and $f_2 = 875$ Hz with the two net modulation depths $\triangle Q_1 \approx 2.5 \cdot 10^{-4}$ and $\triangle Q_2 \approx 5.0 \cdot 10^{-4}$.

In all cases, we measured a widening of the stochastic layers for a modulation with more than one frequency due to an overlap of modulation resonances. For a modulation resonance, the modulation frequency is an integer multiple of the island oscillation frequency. If one considers more than one modulation frequency, neighbouring modulation resonances might overlap and lead to an increase in the width of the chaotic area.

Even though we are far from explaining the SPS experiment quantitatively with our results, we illustrate three qualitative different mechanisms that lead to an increased particle diffusion for more than one modulation frequency. A quantitative explanation of the effects observed in the SPS would clearly demand a more elaborate lattice than our simple model structure, and the insight gained from the work presented here could assist in such a quantitative analysis.

REFERENCES

1. X.Altuna, C.Arimatea, R.Bailey, T.Bohl, D.Brandt, K.Cornelis, C.Depas, F.Galluccio, J.Gareyte, R.Giachino, M. Giovannozzi, Z.Guo, W.Herr, A.Hilaire, T.Lundberg, J.Miles, L.Normann, T.Risselada, W.Scandale, F.Schmidt, A.Spinks, M.Venturini (1991), CERN SL/91-43 (AP), LHC Note 171.
2. B.V. Chirikov (1979) *Physics Reports* **52** 263.
3. A.J. Lichtenberg and M.A. Lieberman, *Regular and Stochastic Motion*, Springer
4. A. Deprit (1969) *Cel. Mech.* **1** 12.
5. E. Courant and H. Snyder (1958) *Annals of Physics* **3** 1.
6. F. Willeke and G. Ripken, DESY 88-114 (August 1988)
7. O. Brüning, HEAC 92
8. B.H. Wiik, DESY Hera 88-05 (April 1988)